FEBS Letters 355 (1994) 297–300

FEBS 14841

Spectroscopic evidence for an intramolecular RNA triple helix

R. Klinck[a], E. Guittet[a], J. Liquier[c], E. Taillandier[c], C. Gouyette[b], T. Huynh-Dinh[b,*]

[a]*Institut de Chimie des Substances Naturelles, CNRS, 91198 Gif-sur-Yvette, France*
[b]*Unité de Chimie Organique, URA CNRS 487 - Institut Pasteur, 75724 Paris, France*
[c]*Laboratoire CSSB, URA CNRS 1430 - Université Paris Nord, 93012 Bobigny, France*

Received 21 September 1994

Abstract A 29-base RNA oligomer has been chemically synthesized and shown to form an intramolecular triple helix in solution at acidic pH. Assignment of the majority of the exchangeable proton NMR resonances demonstrated the Watson–Crick and Hoogsteen base pairings consistent with folding to form pyrimidine–purine–pyrimidine base triplets. FTIR spectroscopy provided independent evidence of base triplet formation, and indicated a predominately C3′-endo sugar pucker. UV absorption as a function of temperature suggested monophasic melting behaviour, which was confirmed by NMR of the imino protons.

Key words: RNA structure; NMR; Triple helix; Oligoribonucleotide synthesis

1. Introduction

Knowledge of the three dimensional structure of RNA provides an important insight into its function. RNA has been shown to exhibit wide structural diversity, including a triple helix form [1] first proposed in 1957 [2]. Triple base interactions, where a standard Watson–Crick base pair interacts with a third base via Hoogsteen pairing, have recently been the subject of renewed interest, notably in investigations of the catalytic domain of group I introns [3]. The potential biological importance of triplet base interactions as structural motifs at the catalytic site of a ribozyme has been reported [4]. Recently, NMR has been used to elucidate the solution structure of several DNA triple helices [5,6], but to date few structural investigations of RNA triplet base interactions have been reported [7,8]. We undertook an NMR study of a model triple helix to further define triplet base interactions and investigate the conformational potential of RNA.

As part of our ongoing interest in oligoribonucleotides [9,10], we synthesized a 29-base oligomer as a model of an RNA triple helix. The sequence chosen was based on the analogous 28-base DNA sequence reported by Sklenar and Feigon [11] with an additional loop nucleotide. This sequence was designed to allow the folding to form an intramolecular triple helix consisting of C+:G:C and U:A:U base triplets at acid pH, as shown in Fig. 1. Although the chemical synthesis of RNA is not as straightforward as that of DNA due to problems introduced by the 2′-hydroxyl group [12], we have demonstrated that the preparation of milligram quantities of pure RNA is feasible for oligomers in the 10 kDa molecular weight range. Chemical synthesis presents the primary advantage over in vitro T7 polymerase transcription in that it affords complete flexibility in the choice of sequence, particularly with respect to the initial 5′-end bases [13]. The use of modified nucleotides is also made possible via chemical synthesis, although the incorporation of ^{13}C and ^{15}N labelled nucleotides has yet to be proven more practicable than enzymatic transcription [14,15].

*Corresponding author. Fax: (33) (1) 45 68 84 04.

2. Materials and methods

2.1. Synthesis

Automated synthesis (Applied Biosystems 380B) of the oligomer was carried out using controlled pore glass support and phosphoramidite chemistry with a *tert*-butyldimethylsilyl (TBDMS) protecting group at the 2′ position (Milligen/Millipore). A 10 μmol scale synthesis gave a total yield of 87% (average coupling yield 99.5%) based on trityl assay. Deprotection was carried out using NH_3 saturated ethanol at 55°C for 24 h followed by 24 h at room temperature. The TBDMS protecting group was removed with tetrabutylammonium flouride/tertahydrofuran (12 ml, 1.1 M) for 48 h at room temperature. The crude product was desalted twice on a Sephadex G-10 column, eluting with 0.1 M then 0.05 M triethylammonium acetate (TEAA). The eluted product, detected by UV absorbance at 260 nm, was lyophilized then purified using preparative HPLC (Nucleosil 300 Å 5-C18 1/2″ × 25 cm; flow rate 5.5 ml/min in 0.01 M TEAA, pH 7, with a 5–25% CH_3CN gradient). The purified product was exchanged with a Dowex 50W-X8 Na+ column then lyophilised to yield 14.6 mg (15.5% total yield purified product). The purity was verified with capillary electrophoresis, analytical HPLC and polyacrylamide gel electrophoresis of a ^{32}P 5′-end labelled sample. The oligonucleotide was completely degraded by snake venom phosphodiesterase.

2.2. NMR spectroscopy

All spectra were recorded at 600 MHz proton frequency on a Brüker AMX 600 instrument. The sample was approximately 1.2 mM oligomer and 20 mM NaCl in 450 μl 10% D_2O 90% H_2O at pH 4.8. One- (1D) and two-dimensional (2D) spectra were acquired with a spectral width of 15 kHz. The 2D nuclear Overhauser effect spectroscopy (NOESY) data set consisted of 2,048 and 200 complex points in t2 and t1, respectively, 160 scans per t1 increment, and quadrature detection using the States [16] method. A 2 ms pulsed field gradient was applied at the end of the 180 ms mixing time and a 235 μs SS pulse [17] was used for detection to avoid excitation of the water resonance. Data were processed with the GIFA software [18], developed in our laboratory. Linear prediction of two additional points at the beginning of the free induction decays was used to correct the linear phase error in f2. The data in t1 were linearly predicted to 512 points. 60° shifted sine squared functions were applied in both dimensions prior to Fourier transform to yield a spectrum of 2048 and 512 real points in f2 and f1, respectively.

2.3. FTIR and UV Spectroscopy

FTIR spectra were recorded on a Perkin Elmer 1760 spectrophotometer, using ZnSe cells. The oligomer was approximately 2 mM in D2O solution and the pH of the 1 μl sample was controlled using a microelectrode. 20 scans were co-added for each spectrum. Data was processed using the Spectracalc software (Galaxy Inc.). The spectra were baseline corrected and normalized. The UV absorbance as a function of temperature was recorded at 262 Å on a Kontron Uvikon 941

SSDI 0014-5793(94)01228-8

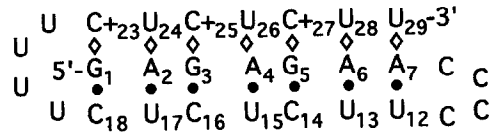

Fig. 1. Sequence and proposed folding of 29-base RNA intramolecular triple helix. (●) Watson–Crick pairing, (◇) Hoogsteen base pairing.

spectrophotometer. The sample was approximately 3 μM oligomer and 20 mM NaCl in H_2O, at pH 4.8.

3. Results

The imino region of the 1D NMR spectrum, and the corresponding region of a NOESY spectrum showing the imino–imino correlations, are presented in Fig. 2a,b. With the exception of $C+_{23}$ and U_{29}, all the imino proton resonances could be observed and were assigned as described below. Sequential imino–imino NOESY crosspeaks, shown in Fig. 2b, were detected for all the observed resonances except U_{24}-$C+_{25}$. In addition to the sequential correlations, conditions favouring spin diffusion revealed U_{26}-G_3, $C+_{27}$-G_5 and U_{28}-G_5, as well as U_{24}-U_{17} and U_{28}-U_{13} imino–imino crosspeaks, which served as strong evidence for the proposed folding.

The absence of the $C+_{23}$ and U_{29} resonances made it impossible to assign the $U_{24}C+_{25}U_{26}C+_{27}U_{28}$ sequence unambiguously based solely on imino–imino nuclear Overhauser effect (NOE)

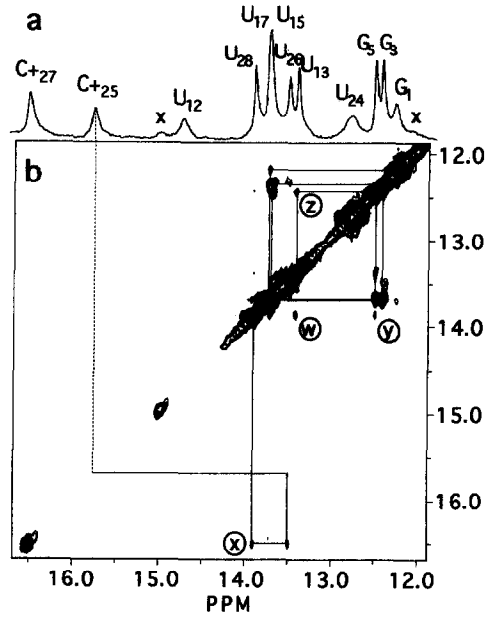

Fig. 2. (a) 1D imino proton spectrum (pH 4.8 and 10°C), and (b) corresponding region of the NOESY (180 ms mixing time) spectrum showing imino–imino correlations. Sequential correlations are joined by lines. The U_{12}-U_{13}, $C+_{27}$-G_5 and U_{24}-U_{17} crosspeaks were observed in a separate experiment at 1°C (not shown). Crosspeaks labelled 'w' to 'z' correspond to the NOEs shown schematically in Fig. 4. (X) indicates unidentified minor peaks, possibly of an alternate conformation.

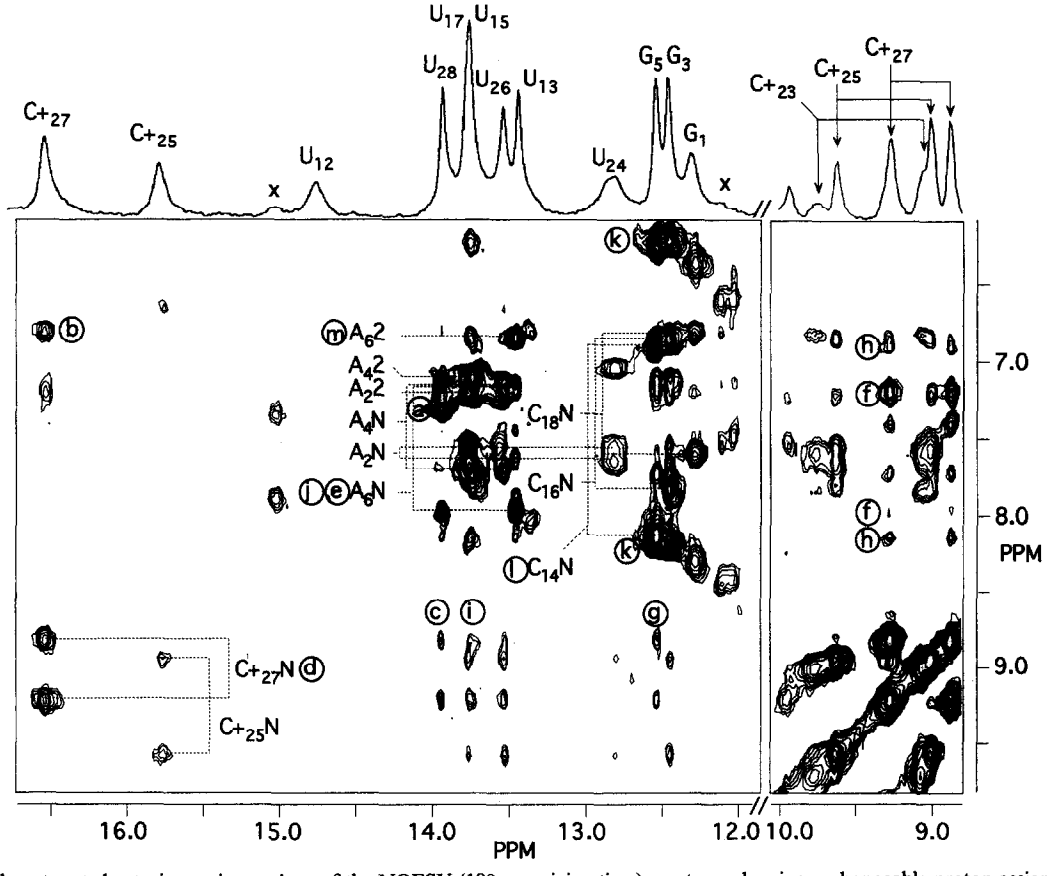

Fig. 3. Imino and protonated cytosine amino regions of the NOESY (180 ms mixing time) spectrum showing exchangeable proton assignments indicative of triple helical structure. Crosspeaks labelled 'a' to 'm' correspond to the NOEs shown schematically in Fig. 4. The spectra were recorded at 10°C, pH 4.8 and 1.2 mM oligomer in 95% H_2O, 5% D_2O. The resonance assigned to U_{12} had completely exchanged with water in the NOESY spectrum.

crosspeaks. The imino to amino and aromatic proton NOEs, presented in Fig. 3, were thus essential for the resolution of this ambiguity. These correlations confirmed the imino proton assignments, and further defined the base triplets. The $C+_{25}$ and $C+_{27}$ amino protons, identified by their strong intranucleotide imino–amino NOEs, showed correlations not only with their Hoogsteen base-paired guanine imino protons, but also with the uracil iminos in the 5′ and 3′ directions and, unique to the triple helix, with the uracil iminos in the 3′ direction on the Watson–Crick paired strand. Of particular interest were the $C+_{25}$-U_{24} amino-imino crosspeaks which provided the basis for the assignment of the broad U_{24} imino resonance. The $C+_{23}$ amino protons were also tentatively assigned based on their similar chemical shift and weak NOEs observed with the U_{24} imino at lower temperature (not shown). The C_{14}, C_{16} and C_{18} amino protons were assigned by their strong NOEs with their Watson–Crick paired iminos. Specific to the C+:G:C base triplet were correlations between these amino protons and those of the protonated cytosines. As expected for a U:A:U base triplet, both Hoogsteen and Watson–Crick base-paired iminos shared correlations with the adenine amino protons.

Imino cross peaks with the aromatic H2, H5 and H8 protons and, consistent with C3′-endo sugar conformation [19], with the H1′ in the 3′ direction and an interstrand H1′, were assigned. These and the other non-exchangeable proton assignments, demonstrating the predominately C3′-endo sugar conformation will be described in detail in a forthcoming paper.

Fig. 4 shows a schematic representation summarizing the NOE correlations observed for, as an example, the $C+_{27}$:G_5:C_{14} and U_{26}:A_6:U_{13} base triplets. The proximities indicated are derived from the NOESY crosspeaks labelled in Figs. 2b and 3, and represent both direct and indirect (i.e. via spin diffusion) correlations.

The UV melting curve is presented Fig. 5a. The single transition observed at 63 °C can be interpreted as a simultaneous melting of the Watson–Crick and Hoogsteen base pairs. These results were consistent with the NMR analysis of the imino proton spectrum as a function of temperature, presented in Fig. 5b. As the temperature increases, the rate of exchange of the imino protons with water can be seen to increase, as indicated by the progressive disappearance of the peaks. As for the single

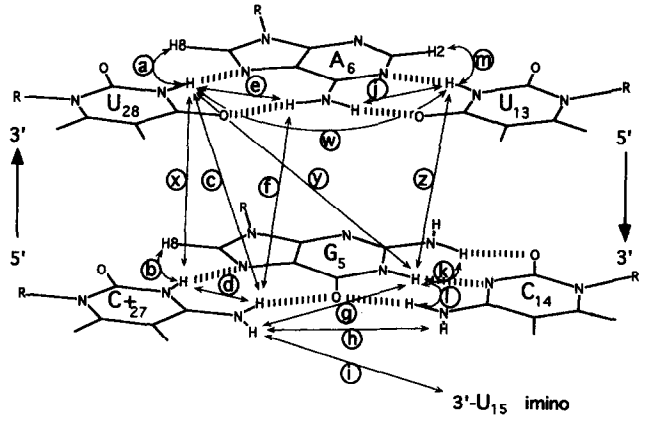

Fig. 4. Schematic representation summarizing the interproton NOEs observed for the $C+_{27}$:G_5:C_{14} and U_{26}:A_6:U13 base triplets. The spin diffusion pathways are not indicated. Double headed arrows indicate NOESY correlations labelled in Figs. 3 ('a' to 'm') and 2b ('w' to 'z'). Dashed lines show the proposed hydrogen bonding.

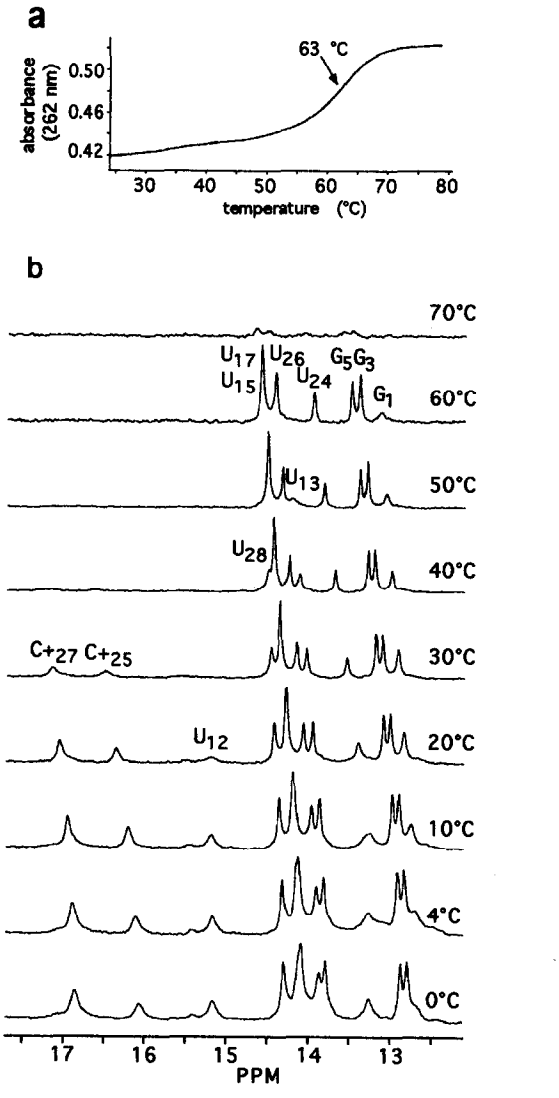

Fig. 5. (a) UV absorbance at 262 nm as a function of temperature. (b) Proton spectra of the imino resonances as a function of temperature. Assignments are indicated for the resonances at the highest temperature at which they were observed.

transition observed in UV melting curve at pH 4.8, this increased rate of exchange occurs roughly simultaneously on Hoogsteen and Watson–Crick paired strands and can be interpreted as a general opening of the base triplets from the loop junctions towards the centre of the proposed triple helix. The stability of the triple helix is illustrated at 60°C, where the seven imino resonances remaining include the U_{24}-A_2-U_{17} and U_{26}-A_4-U_{15} base triplets.

FTIR spectroscopy of the oligomer provided independent confirmation of triple helical structure. The spectra of the 29-mer recorded in D_2O at pH 4.8 and 7.9, presented in Fig. 6, were consistent with the presence of a triple helix at the lower pH. The higher pH value was chosen to ensure that no protonated cytosine residues were likely to be present. An absorption observed at 1,705 cm^{-1} is characteristic of C+:G:C triplets [20], and disappearance of the adenine absorption around 1,633 cm^{-1} at acidic pH has been shown to indicate the presence of U:A:U triplets [21]. The sugar geometries in nucleic acid dou-

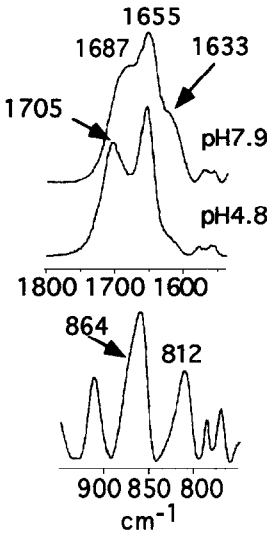

Fig. 6. FTIR spectra in D_2O solution at pH 7.9 and 4.8, showing absorptions characteristic of base triplets (top), and at pH 4.8 showing the absorptions characteristic of C3′-endo sugar conformation (bottom).

ble and triple helices are characterized by IR marker bands in the 1,000–800 cm^{-1} region [22]. C3′-endo type geometry is characterised by absorptions located around 860 cm^{-1} and 810 cm^{-1} while C2′-endo type sugar pucker is characterised by an absorption around 830 cm^{-1} . Thus the absorptions observed at 864 cm^{-1} and 812 cm^{-1} at both pH values are characteristic of the C3′-endo type conformation . The absence of an absorption around 830 cm^{-1} suggests that there is no C2′-endo sugar conformation present.

4. Discussion

Considering the limited intramolecular folding possibilities of the 29-mer sequence, the exchangeable proton and FTIR spectral data are consistent with the simultaneous proximity of two pyrimidine strands to a single purine strand, and provide conclusive evidence for the postulated triple helix motif.

The long NOESY mixing time used revealed spin diffusion pathways which were unique to triple helical structure. For example, the correlations labeled 'g' and 'w' in Fig. 4 arise most likely by transfer through the intervening amino protons, clearly demonstrating the existence of the base triplets.

The monophasic melting behavior reported here has also been reported for similar DNA triple helices [23,24]. A major difference between the DNA and RNA oligomers however appears to be the sugar pucker of bases involved in the triple helix. Whereas our FTIR and preliminary NMR data suggest C3′-endo sugar conformation, Feigon and co-workers concluded that their intramolecular DNA triple helix contained predominately C2′-endo sugar conformations [24]. We are further investigating these differences using chimaeric DNA–RNA oligonucleotides.

Physical evidence of RNA triple helical structure, indicating its relatively high stability in solution, lends support to its proposed role in biological processes and opens the way for a more detailed study of the structural implications of RNA triplet-base interactions. We are currently using multidimensional homo- and hetero-nuclear NMR to assign the non-exchangeable protons of the 29-mer, with the aim of characterizing the conformational requirements of RNA nucleotides involved in base triplets of this type.

References

[1] Saenger, W. (1984) Principles of Nucleic Acid Structure, Springer-Verlag, New York.
[2] Felsenfeld, G., Davies, D.R. and Rich, A. (1957) J. Am. Chem. Soc. 79, 2023–2024.
[3] Michel, F., Ellington, A.D., Couture, S. and Szostak, J. W. (1990) Nature 347, 578–580.
[4] Michel, F. and Westhof, E. (1990) J. Mol. Biol. 216, 585–610.
[5] Rajagopal, P. and Feigon, J. (1989) Nature 339, 637–640.
[6] de los Santos, C., Rosen, M. and Patel, D. (1989) Biochemistry 28, 7282–7289.
[7] Chastain, M. and Tinoco Jr., I. (1992) Biochemistry 31, 12733–12741.
[8] Chastain, M. and Tinoco Jr., I. (1993) Biochemistry 32, 14220–14228.
[9] Ceolin, F., Babin, F., Huynh-Dinh, T., Igolen, J., Bloch, J., Tran Dinh, S. and Neumann, J. M. (1987) J. Am. Chem. Soc. 109, 2939–2941.
[10] Bloch, G., Ceolin, F., Macquaire, F., Neumann, J.M., Babin, F. and Huynh-Dinh, T. (1989) J. Biomol. Struct. Dyn. 6, 1151–1175.
[11] Sklenár, V. and Feigon, J. (1990) Nature 345, 836–838.
[12] Ogilvie, K.K., Usman, N., Nicoghosian, K. and Cedergren, R.J. (1988) Proc. Natl. Acad. Sci. USA 85, 5764–5768.
[13] Milligan, J.F., Groebe, D.R., Witherell, G.W. and Ulenbeck, O.C. (1987) Nucleic Acids Res. 15, 8783–8798.
[14] Batey, R.T., Inada, M., Kujawinski, E., Puglisi, J.D. and Williamson, J.R. (1992) Nucleic Acids Res. 20, 4515–4523.
[15] Nikonowicz, E.P., Sirr, A., Legault, P., Jucker, F.M., Baer, L.M. and Pardi, A. (1992) Nucleic Acids Res. 20, 4507–4513.
[16] States, D.J., Haberkorn, R.A. and Ruben, D.J. (1982) J. Magn. Reson. 48, 286–291.
[17] Smallcombe, S. (1993) J. Am. Chem. Soc. 115, 4776–4785.
[18] Delsuc, M.A., Stoven, V. and Robin, M. (unpublished).
[19] Heus, H.A. and Pardi, A. (1991) J. Am. Chem. Soc. 113, 4360–4361.
[20] Ouali, M., Letellier, R., Adnet, F., Liquier, J., Sun, J., Lavery, R. and Taillandier, E. (1993) Biochemistry 32, 2098–2103.
[21] Liquier, J., Coffinier, P., Firon, M. and Taillandier, E. (1991) J. Biomol. Struct. Dyn. 9, 437–445.
[22] Taillandier, E. and Liquier, J. (1992) Methods Enzymol. 211 (DNA Struct. Part A), 307–335.
[23] Wang, E., Malek, S. and Feigon, J. (1992) Biochemistry 31, 4838–4846.
[24] Macaya, R., Wang, E., Schultze, P., Sklenar, V. and Feigon, J. (1992) J. Mol. Biol. 225, 755–773.